Effect of Metal−Ligand Mutations on Phosphoryl Transfer Reactions Catalyzed by *Escherichia coli* Glutamine Synthetase†

Lynn M. Abell,*,‡ Jeffrey Schineller,§ Pamela J. Keck,|| and Joseph J. Villafranca*,⊥

Department of Chemistry, The Pennsylvania State University, University Park, Pennsylvania 16802

Received June 14, 1995; Revised Manuscript Received October 4, 1995®

ABSTRACT: Glutamine synthetase (GS) converts glutamate to glutamine in the presence of ATP and ammonia and requires two divalent metal ions, designated n_1 and n_2, for catalysis. The first intermediate, γ-glutamyl phosphate, is formed during catalysis by the transfer of the γ-phosphate of ATP to the γ-carboxylate of glutamate. Efficient phosphoryl transfer between these two negatively charged moieties is thought to be mediated by the n_2 metal. To explore the role of the n_2 metal in catalysis, histidine 269, a ligand to the n_2 metal, was changed to aspartate, asparagine, glutamate, and glutamine by site-directed mutagenesis. All of the mutants bind two manganese ions as determined by EPR titration. The mutations had little effect on the substrate K_m's except in the case of H269E which exhibited a $K_{m\ Glu} = 92$ mM, a 1000-fold increase compared to that for WT ($K_{m\ Glu} = 70\ \mu$M). The ability of these mutants to catalyze phosphoryl transfer to glutamate or to the inhibitor phosphinothricin was examined by rapid quench kinetic experiments. Phosphorylated phosphinothricin was detected by ^{31}P NMR and shown to be produced by both mutants and WT. The rate of phosphoryl transfer to PPT for H269E is reduced 100-fold (0.030 s^{-1}) compared to WT (8 s^{-1}). The extra negative charge around the n_2 metal ion contributed by glutamate 269 severely reduces the ability of the n_2 metal to mediate efficient glutamate binding in the presence of negatively charged ATP and weakens the interactions between metal ion and the reactants in the transition state, thus resulting in a lower rate of phosphoryl transfer.

Glutamine synthetase (GS)[1] from *E. coli* catalyzes the ATP-dependent formation of glutamine from glutamate and ammonia.

$$\text{Glutamate} + \text{ATP} + \text{NH}_3 \xrightleftharpoons{2\ M^{2+}} \text{Glutamine} + \text{ADP} + \text{Pi}$$

The enzyme requires two divalent metal ions for catalysis which are distinguished from one another by their dissociation constants. The more tightly bound n_1 metal ion is required to keep the enzyme in its catalytically active conformation while the less tightly bound n_2 metal ion is thought to facilitate nucleotide binding. The protein ligands to these metal ions are known from the crystal structure of the enzyme from *Salmonella typhimurium* which differs from the *E. coli* enzyme by six conservative amino acid changes (Almassey et al., 1986; Yamashita et al., 1989). The n_1 metal ion has three glutamate side chains—131, 212, and 220—as ligands, while the n_2 metal ion has two glutamate ligands, 129 and 357, as well as histidine 269. All of the amino acids that serve as metal ion ligands are highly conserved in glutamine synthetases from various sources (Pesole et al., 1991).

The first chemical step catalyzed by glutamine synthetase involves the transfer of the γ-phosphoryl group of ATP to the γ-carboxyl group of glutamate. Model studies of phosphoryl transfer reactions in solution have indicated that while there is little electrophilic catalysis during phosphoryl transfer by metal ions such as Mg^{2+} (Herschlag & Jencks, 1987), the metal ion provides a template to orient substrates and to assist the departing leaving group (Herschlag & Jencks, 1989). In addition to properly orienting the substrates, metal ions have often been thought of as electropositive centers that shield the negative charges of the anionic groups that would otherwise repel each other (Jencks, 1969) as would be the case for the γ-carboxyl group of glutamate and the γ-phosphoryl group of ATP.

One approach to examining the role of the metal ion in reactions catalyzed by GS is to alter the metal ion ligands by site-directed mutagenesis. In these studies histidine-269 was replaced by asparagine, aspartate, glutamate, and glutamine. This series of mutations provides both neutral and negative side chains to interact with the metal ion. The effect of these mutations on metal binding, intrinsic enzyme fluorescence, and on the dissociation constant for ATP was examined.

The effect of the histidine-269 mutations on the metal ion required for catalysis was also examined and the effect of adenylylation on these mutants was determined by studying mutants with various states of adenylylation. Adenylylation

† This work was supported by NIH Grants GM23529 (J.J.V.) and GM11994 (L.M.A.).

* Corresponding authors.

‡ Current address: Du Pont Agricultural Products, Stine-Haskell Research Center, P.O. Box 30, Elkton Road, Newark, DE 19714.

§ Current address: Department of Biochemistry and Biophysics, Texas A&M University, College Station, TX 77843.

|| Current address: Monsanto Agricultural Co., Chesterfield, MO 63198.

⊥ Current address: Pharmaceutical Research Institute, Department of Macromolecular Research, Bristol-Myers Squibb, P.O. Box 4000, Princeton, NJ 08543.

® Abstract published in *Advance ACS Abstracts,* December 1, 1995.

[1] Abbreviations: GS, glutamine synthetase; WT, wild type; *n*, average adenylylation state; PPT, L-2-amino-4-(hydroxymethylphosphinyl)butanoic acid; PPT-P, phosphinothricin phosphate; Hepes, *N*-(2-hydroxyethyl)piperazine-*N*′-2-ethanesulfonic acid; PEP, phosphoenol pyruvate; EDTA, ethylenediaminetetraacetic acid; Pipes, piperazine-*N*,*N*′-bis(2-ethanesulfonic acid); EPR, electron paramagnetic resonance.

0006-2960/95/0434-16695$09.00/0

of WT occurs *in vivo* and serves to regulate the activity of the dodecamer. This modification involves the reversible covalent attachment of an adenyl group to Tyr-397 by the enzyme adenyl transferase in response to the level of glutamine and α-ketoglutarate in the cell (Reitzer & Magasanik, 1987). The effect of adenylylation on the kinetics of the WT is to elevate the K_m's for all substrates (Abell & Villafranca, 1991a) and to change the metal ion specificity and pH required for optimal activity. The unadenylylated enzyme shows optimal activity with Mg^{2+} at pH 7.5 while the adenylylated enzyme exhibits maximal activity with Mn^{2+} at pH 6.5.

In order to examine the role of the histidine-269 mutations on the phosphoryl transfer step, rapid quench kinetic experiments were conducted on the mutants. Rapid quench kinetic experiments have been conducted on several different forms of WT in the presence of ATP, glutamate, and ammonia in order to detect the presence of the γ-glutamyl phosphate intermediate (Meek et al., 1982) as well as to determine the effect of metal ion type and adenylylation state on phosphoryl transfer (Abell & Villafranca, 1991a). The later studies showed that regardless of which metal ion is used, Mn^{2+} or Mg^{2+}, product release is rate-limiting for WT $n = 2$. However, with fully adenylylated enzyme, phosphoryl transfer is rate-limiting.

Previously, rapid quench experiments have been conducted on WT in the presence of the inhibitor phosphinothricin (Abell & Villafranca, 1991b). Phosphinothricin is a slow-binding inhibitor of glutamine synthetase which resembles the tetrahedral intermediate. The inhibitor requires ATP for inactivation and undergoes phosphorylation during the course of inactivation to produce ADP and acid-labile PPT-P. A tightly bound complex is formed between ADP and phosphorylated phosphinothrincin during inactivation.

EXPERIMENTAL PROCEDURES

Materials. [α-^{35}S]ATP for sequencing was from New England Nuclear. Restriction enzymes were from New England BioLabs. Sequencing was conducted using either reverse transcriptase from Promega or Sequenase from US Biochemical Corporation. All other biochemicals were from Sigma Chemical Company and were of the highest purity available. [γ-^{32}P]ATP (10−50 Ci/mmol) was obtained from New England Nuclear and purified prior to use according to Lewis and Villafranca (1989). Phosphinothricin (D,L) was a gift from Hoechst. Concentrations given for PPT refer to the L isomer throughout. All other biochemicals were from Sigma and were of the highest purity available.

Mutagenesis. H269N and H269D were constructed using M13 subclones of *glnA*, the structural gene for glutamine synthetase and the method of Kunkel et al. (1991). The following oligonucleotides were used: His → Asn-269, 5′-GAT AAC GGA TCC GGT ATG AAC TGC CAC-3′; His → Asp-269: 5′-GAT AAC GGA TCC GGT ATG GAC TGC CAC-3′. Mismatched bases are underlined. A second silent mutation was contained in each oligo in which GGC was replaced by GGA. This mutation added a *BamHI* restriction site for screening purposes. The mutation was confirmed by single-stranded sequencing. For construction of H269E and H269Q the method of Sayers and Eckstein (1988) was used via the Amersham kit. *GlnA* was cloned into pTZ18R (pBL88), and this plasmid was used to obtain single-stranded DNA for mutagenesis by infection of RZ1032 harboring this plasmid with helper phage M13KO7. A single oligo was used for both mutations which contained a 50/50 G/C wobble: His → Glu-269 and His → Gln-269, 5′-AAC GGC TCC GGC ATG (C/G)AA TGC CAC ATG-3′. The oligo also contained a silent mutation of GGT to GGC. This mutation allowed for screening of mutants by restriction digestion. Colonies from mutagenesis experiments could be screened for mutations initially by looking for reduced activity compared to WT activity using the γ-glutamyl transferase assay (Woolfolk et al., 1966). Those that showed reduced activity could then be distinguished from one another by *Sph*I digestion. H269Q contained an extra *Sph*I site due to the silent mutation. Mutations were confirmed by double-stranded sequencing.

The mutations were ultimately subcloned into pgln35 for expression (Backman et al., 1981). This plasmid contains the *glnALG* operon, where *glnG* codes for NR_I, a transcriptional enhancer for GS, and *glnL* encodes NR_{II}, a transcriptional regulator (Reitzer & Magasanik, 1987). The plasmid contains a 480 bp deleton in *glnL* which results in elimination of ammonia repression of transcription (Ninfa & Magasanik, 1986). The *glnA* region of the plasmid was completely sequenced after subcloning to confirm the presence of only the desired mutation. The mutant plasmids were placed in YMC11, a strain of *E. coli* which is deficient in WT glutamine synthetase (Backman et al., 1981). This construct produced 150−250 mg of enzyme from 25−40 g of cells.

Enzyme. WT $n = 2$ and WT $n = 12$ were prepared as previously described (Abell & Villafranca, 1991a). YMC11/plgn35 mutants were grown on minimal media with glucose as the carbon source and glutamine as the sole nitrogen source. In the final growth, $MnCl_2$ was added to a final concentration of 1 mM to inhibit oxidation of GS (Roseman & Levine, 1987). Cells were harvested after reaching late log phase. Mutants were purified using the same method as WT which was a variation of the zinc precipitation method (Miller et al., 1974) and included a streptomycin sulfate step, one zinc precipitation step followed by extensive dialysis to remove the zinc, an acetone precipitation step at 0 °C, and a final ammonium sulfate precipitation at pH 4.4 (Rhee et al., 1985). Protein concentrations were determined by the BCA assay (Pierce) in the absence of Mn^{2+}.

The adenylylation state of the mutants was determined by acid hydrolysis of the protein followed by phosphate determination. Several protein samples containing 0.25−0.75 mg of enzyme were prepared in approximately 100 μL of 10 mM imidazole, 100 mM KCl, and 1 mM $MnCl_2$ at pH 7.2. Concentrated HCl (40 μL) was added and the sample was boiled for 30 min. The sample was diluted to a total final volume of 500 μL and assayed for phosphate using the method of Lanzetta et al. (1979). The number of moles of phosphate present and the total amount of enzyme could then be used to calculate the adenylylation state.

Completely adenylylated mutants were prepared *in vitro* using the enzyme adenylyl transferase (Hennig & Ginsburg, 1971) and then repurified by zinc precipitation and an ammonium sulfate precipitation. After purification, mutants were stored at 4 °C in 1 mM $MnCl_2$, 20 mM imidazole, 100 mM KCl at pH 7.2.

Preparation of Low Adenylylation State Enzyme. The adenylylation state of mutants varied even when grown under conditions that normally produced low adenylylation state

WT. Therefore, in those cases where mutants with high adenylylation states were obtained, i.e., H269D, the enzyme was deadenylylated using snake venom phosphodiesterase (PDE) (Atkins et al., 1991). The yield from this procedure varied depending on the mutant. A 70% yield was obtained for H269N, but only a 30% yield was obtained with H269D.

EPR Measurements. EPR titration experiments were carried out at 25 °C with a Varian E-12 spectrophotometer at 9 GHz. Apoenzyme was prepared by dialysis against 50 mM imidazole, 100 mM KCl, and 2 mM EDTA, at pH 7.2 for 12 h followed by exhaustive dialysis (36+ h) against the same buffer in the absence of EDTA. Mn^{2+} solutions were prepared fresh in imidazole/KCl buffer and were standardized by titration with an arsenazo/pyridine solution against a Mn^{2+} atomic absorption standard (Sigma). The height of the first two peaks in the Mn^{2+} EPR sextet was used to determine the amount of free Mn^{2+} in each sample. The resulting data were fit by nonlinear regression analysis to a two-site binding model, eq 1:

$$\nu = \frac{[Mn]_b}{[E]_t} = \frac{K_1[Mn]_f}{1 + K_1[Mn]_f} + \frac{K_2[Mn]_f}{1 + K_2[Mn]_f} \quad (1)$$

where $[Mn]_f$ and $[Mn]_b$ are the concentration of free and bound Mn^{2+} and K_1 and K_2 are the association constants for the first and second sites. Remaining apoenzyme was reconstituted with Mn^{2+} and checked for activity.

Fluorescence Measurements. Fluorescence titration experiments were carried out at 25 °C in 1 cm quartz cuvettes on a Perkin-Elmer MPF-44B fluorescence spectrophotometer. The excitation wavelength was 300 nm, and emission was monitored at 336 nm. Titrations were conducted using the Mn^{2+} form of the enzymes and buffer which contained 100 mM Pipes, 100 mM KCl, and 8 mM $MnCl_2$ at pH 6.5. The enzyme concentration utilized in these experiments was typically 1−5 μM in unadenylylated subunits. The titrant contained ATP in the buffer described above as well as enzyme with a concentration equilvalent to that in the cuvette in order to minimize dilution effects during titrant addition. The resulting data were fit to eq 2:

$$\Delta F = \Delta F_{max} - K_D(\Delta F/[L]) \quad (2)$$

where ΔF is the change in fluorescence observed upon addition of titrant, ΔF_{max} is the final total change in fluorescence, K_D is the dissociation constant, and [L] is the concentration of ligand. Linear regression analysis of plots of ΔF vs. $\Delta F/[L]$ provided values of K_D.

Steady-State Kinetics. The biosynthetic activity at pH 6.5 and 7.5 using either Mg^{2+} or Mn^{2+} as the activating metal ion was monitored spectrophotometrically by coupling ADP production to NADH oxidation using lactate dehydrogenase and pyruvate kinase. The assay mix contained 100 mM Hepes, 100 mM Pipes, 100 mM KCl, 1 mM PEP, 190 μg of NADH, 33 μg/mL of pyruvate kinase, and 33 μg/mL of L-lactate dehydrogenase. The amount of metal required for optimal activity was determined for each enzyme at a given pH by holding [ATP] and [glutamate] constant and varying the metal ion concentration. When the optimal concentration was determined, a fixed concentration of excess metal ion over ATP was held constant when ATP concentration was varied (Morrison, 1979).

The K_m's for ATP and glutamate were determined by varying the concentration of one of the substrates while holding the other fixed at 5−10 times the K_m value. The ammonia concentration was held constant throughout at 50 mM. Assays were performed in 1.0 cm cuvettes with 1.00 mL total volume in a Cary 2200 UV/VIS spectrophotometer thermostatted at 25 °C. The change in absorbance at 340 nm vs. time was monitored. Initial rates of reaction were determined using SPECTRA CALC.

Steady-state kinetic data were analyzed using the computer programs of Cleland (1979) modified for the MacIntosh computer. Data from kinetic experiments with the Mg^{2+} form of H269N fit best to eq 3 for an equilibrium ordered mechanism.

$$y = \frac{VAB}{K_{ia}K_b + K_bA + AB} \quad (3)$$

Rapid Quench Experiments. Rapid quench experiments were performed with an apparatus designed and built by Johnson (1986). The reactions were initiated by the simultaneous mixing of two solutions; one containing enzyme and activating metal ion at the appropriate pH (0.039 mL), and the other containing all substrates and metal ions (0.042 mL) as well as trace amounts of [γ-^{32}P]ATP (5000 cpm/nmol of cold ATP). The reactions were quenched with 190 μL of 0.6 N HCl and then immediately neutralized with 45 μL of a solution containing 1 M Tris and 4 N KOH. [γ-^{32}P]Pi was isolated as described by Johnson (1986). Cold ATP concentrations were determined spectrophotometrically by measuring the absorbance at 259 nm of a 0.1 M solution prepared from the stock solution. In addition to substrates and enzyme, each final reaction mixture contained 100 mM Pipes, 100 mM KCl, 8 mM $MnCl_2$, 1 mM PEP, and 33 μg/mL of pyruvate kinase at pH 6.5.

Biosynthetic Reactions. All biosynthetic rapid quench experiments were conducted at 10 °C. Enzymes were dialyzed into this buffer system containing the appropriate metal ion concentration prior to each reaction (see above). For H269N, the final reaction mixture contained 35.6 μM unadenylylated subunits, 490 μM ATP, 375 μM glutamate, and 50 mM NH_4Cl. For H269Q, the final reaction mixture contained 29.3 μM unadenylylated subunits, 471 μM ATP, 379 μM glutamate, and 50 mM NH_4Cl.

Experiments with PPT. All reactions were carried out at 25 °C. For H269N and H269Q, the final reaction mixture contained 600 μM ATP, 100 mM PPT, and micromolar amounts of enzyme. Data were collected from 5 ms to 4 s. For H269E, the final reaction mixture contained 600 μM ATP, 270 mM PPT, and micromolar amounts of enzyme. Higher concentrations of PPT were used in the case of H269E because of the slow inactivation rate observed in preincubation experiments, 18 M^{-1} s^{-1}, which is several orders of magnitude slower than the 10^3 M^{-1} s^{-1} inactivation rate observed for WT (Abell and Villafranca, unpublished results). H269N and H269Q showed inactivation rates comparable to or faster than WT. Data was collected from 5 ms to 60 s. At these high concentrations of PPT, the association rate of the inhibitor with the enzyme−ATP complex should be fast, and only the phosphoryl transfer rate should be measureable. Because of the slow ATPase reaction exhibited by these mutants in steady-state experiments, control experiments were conducted using labeled

Scheme 1

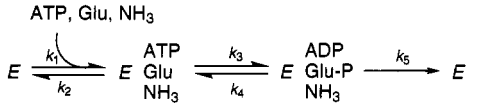

ATP in the absence of PPT. No radiolabeled phosphate release was detected in these experiments in the millisecond time scale for H269N and H269Q or the second time scale for H269E.

Trapping of PPT-P–Mg^{2+} Activated WT. A concentrated sample of WT $n = 2$ (650 μM subunit concentration; 700 μL) in 100 mM KCl, 25 mM $MgCl_2$, 50 mM Hepes buffer at pH 7.5, was inactivated with 2 mM PPT and 4 mM ATP at 25 °C for 30 min. The solution was quenched by the addition of 0.5 mL of triethylamine (Anderson et al., 1988) and one drop of carbon tetrachloride. The reaction solution was centrifuged for 15 min at 14 000 rpm in a microfuge to pellet the denatured enzyme. An aliquot (600 μL) of the aqueous supernatant was filtered through glasswool into a 5 mm NMR tube along with 100 μL of D_2O and 50 μL of a 0.5 M EDTA–K^+ solution (pH 10).

Trapping of PPT-P–Mn^{2+} Activated Enzyme. The formation of phosphinothricin-phosphate was demonstrated for WT, H269N, H269Q, H269E, and H269D in the presence of Mn^{2+} in a manner similar to that described for WT activated with Mg^{2+}. Enzyme (20 mg) was reacted with 2 mM PPT and 4 mM ATP in the presence of 300 mM Pipes, 100 mM KCl, and 8 mM $MnCl_2$ at pH 6.5 in a total volume of 800 μL. The reaction was allowed to proceed at room temperature for 30 min for H269N and H269Q and 3 h for H269E. In the case of H269E, the procedure was modified by the addition of 2 mM PEP and 5 units of pyruvate kinase to regenerate any hydrolyzed ATP that might be formed over the long reaction time. The triethylamine quenching procedure removed the majority of the Mn^{2+}, and the resulting ^{31}P NMR spectra had narrow linewidths.

Data Analysis. Biosynthetic rapid quench data were fit to eq 4 by a nonlinear least squares method:

$$P_i/E = A(1 - e^{-\lambda t}) + k_{ss}t \quad (4)$$

where P_i = (μM) concentration of radioactive inorganic phosphate, E = concentration of unadenylylated subunits/reaction, A = burst amplitude, k_{ss} = steady-state rate constant, λ = transient phase rate constant, and t = time. The rate constants for individual steps in the biosynthetic reaction can be represented as shown in Scheme 1. In this scheme, k_3 represents the phosphoryl transfer step and k_5 includes the ammoniolysis step as well as product release steps. Since the substrate concentrations were saturating in each experiment and, therefore, the association rates for substrates are presumably fast, k_3, k_4, and k_5 may be related to the experimentally determined values from the rapid quench experiments as follows: $k_{ss} = k_3k_5/(k_3 + k_4 + k_5)$, $A = k_3(k_3 + k_4)/(k_3 + k_4 + k_5)^2$, $\lambda = k_3 + k_4 + k_5$.

Rapid quench data with PPT were fit to eq 5 using a nonlinear least squares algorithm:

$$P_i/E = B(1 - e^{-Ct}) \quad (5)$$

where P_i, E, and t are the same as in eq 4, $B = k_6/(k_6 + k_7)$, $C = k_6 + k_7$, k_6 represents the forward phosphoryl transfer rate, and k_7 represents the reverse phosphoryl transfer rate.

Scheme 2

Table 1: Mn^{2+} Dissociation Constants

enzyme	K_1 (μM)	K_2 (μM)
H269D $n = 10$	<0.5 ± 1.0	2.0 ± 1.0
WT $n = 2$[a]	0.5 ± 1.0	45 ± 5
WT $n = 12$	5.0 ± 2.0[b]	100[c]
H269N $n = 6$	5.0 ± 1.0	154 ± 24
H269N $n = 12$	3.5 ± 1.4	142 ± 40
H269Q $n = 5$	11.0 ± 2.0	200 ± 50
H269E $n = 3$	5.0 ± 1.0	55 ± 10

[a] Villafranca et al. (1976). [b] In agreement with that previously measured by Villafranca and Wedler (1974). [c] Denton and Ginsburg (1969).

The internal equilibrium constant for phosphoryl transfer, k_6/k_7, may also be calculated. Equation 5 was derived for the mechanism shown in Scheme 2, which assumes that ATP and PPT binding are fast and acid-labile phosphate formation is due solely to the rate of phosphoryl transfer. At the high concentrations of PPT and the saturating concentrations of ATP used in these experiments, this assumption should be valid.

RESULTS AND DISCUSSION

The physical properties of the H269 mutants were examined to determine the effect of the mutations on (1) the gross integrity of the enzyme conformation especially in the ternary complex, and (2) the physical properties most likely to be affected by a mutation of a metal ion ligand. From the examination of fluorescence changes for the mutants compared to WT in the presence of saturating ATP, metal ion, and glutamate, H269E, H269N, and H269Q, all show fluorescence changes comparable to WT. These observations were taken as an indication that at least in the ternary complex, the conformation of the mutant enzymes is not greatly altered compared to WT. It was also found that these mutants still bound two metal ions although there are no clear patterns correlating the dissociation constants and the type of mutation, neutral versus charged (Table 1). The replacement of histidine-269 with neutral ligands such as asparagine and glutamine altered the dissociation constants three- to fourfold, while substitution with glutamate decreased the dissociation constant slightly. The absence of a correlation between the metal ion dissociation constants and the type of mutation at the position 269 may reflect the primary importance of glutamates 129 and 357 in metal binding and indicate that the neutral histidine plays a lesser role in determining the magnitude of the dissociation constant. The crystal structure of H269N demonstrates that weaker binding constant for Mn^{2+} at the n_2 site results in reduced occupation of the n_2 position by Mn^{2+} in the crystal (Liaw et al., 1993); the rest of the protein structure is not altered by the histidine to asparagine mutation.

ATP binding is also not affected greatly by the mutations (Table 2). This result may be a reflection of the fact that ATP has many other interaction points with the protein other than through the metal ion and that these interactions, rather than binding to the metal ion, play a substantial role in determining the dissociation constant for ATP.

H269D has anomalous properties with respect to WT with regard to both the fluorescence changes observed in the

Table 2: Dissociation Constants for ATP

enzyme	K_D ATP (μM)
H269N $n = 6$	40 ± 2
WT $n = 12$	18 ± 1
H269Q $n = 5$	3.2 ± 0.1
WT $n = 2$[a]	2.5 ± 0.1
H269E $n = 3$	0.9 ± 0.2
H269D $n = 10$	11 ± 0.5

[a] Abell and Villafranca (1991).

presence of substrates and in terms of the metal ion dissociation constants. The fluorescence intensity changes for this enzyme are much less than those observed for WT or any of the other mutant enzymes, and the dissociation constants for Mn^{2+} are much smaller (Table 1). The full implication of these altered properties is revealed in studies of the kinetic behavior of the mutant (Table 4). Both the low and high adenylylation state H269D did not produce glutamine but proved to be a glutamate-independent ATPase. The hydrolysis of ATP to ADP in the presence of glutamate but in the absence of ammonia has long been known to be catalyzed by GS but at 0.1 times the rate of the normal glutamine-forming reaction. A much slower ATPase reaction in the absence of glutamate and ammonia at about 0.01 times the rate of the normal reaction has also been measured for WT (Abell and Villafranca, unpublished results). For H269D, however, the rate of ADP production measured in the coupled assay remained unchanged whether it was measured in the absence of ammonia or in the absence of both ammonia and glutamate. The enzyme requires Mn^{2+} for activity and shows normal hyperbolic kinetics with ATP as the substrate. The k_{cat} for H269D, based on unadenylylated subunit concentration, did not change even though the adenylylation state changed from 2 to 10 (Table 4). Communication between the site of adenylylation and the active site would appear to be disrupted in this mutant.

It is tempting to speculate on the structural repercussions that might occur upon replacement of histidine with aspartic acid. The negatively charged aspartic acid side chain is expected to have a stronger interaction with the metal ion than does the neutral histidine side chain. This stronger interaction may serve to "pull" the polypeptide backbone closer to the n_2 metal. Presumably this interaction could effectively close off the active site, preventing the transfer of the γ-phosphate group of ATP to glutamate. Another attractive possibility is that the γ-phosphate of ATP is transferred to the β-carboxylate of aspartic acid-269 and that the aspartyl phosphate is then hydrolyzed to produce ADP and inorganic phosphate. Further studies would be required to determine if this is the case.

Steady-State Kinetic Parameters—H269N. Of the mutants, only H269N shows significant activity with either Mg^{2+} or Mn^{2+} as the activating metal ion in the biosynthetic assay. The Mg^{2+} activated H269N has a greatly increased K_m for glutamate and a k_{cat} that is 10-fold lower than that for WT (Table 3). The double reciprocal plots with ATP as the varied substrate at different fixed levels of glutamate resulted in a pattern that intersected to the left of the *Y*-axis. Double reciprocal plots with glutamate as the varied substrate intersect on the *Y*-axis. A replot of the slopes from reciprocal plots vs 1/ATP go through the origin within experimental error. Analysis of these data using eq 3 yields the dissociation constant for ATP. Attempts to fit these data to an equation for a sequential ordered mechanism led to a value of K_a equal to zero within experimental error ($K_a = 0.011 \pm 0.017$) and to larger statistical errors in the overall fit. These results are consistent with a rapid equilibrium sequential mechanism with ATP binding first. The kinetic mechanism for WT is an ordered mechanism, with ATP binding first followed by glutamate and ammonia (Meek & Villafranca, 1980). The mutation has thus altered the kinetic mechanism.

Table 3: Kinetic Parameters for H269N with Mg^{2+}

enzyme	K_{iaATP} (mM)	K_{mATP} (μM)	K_{mGlu} (mM)	k_{cat} (s^{-1})
WT $n = 2$[a]	–	150 ± 7	3.3 ± 0.6	33 ± 3
H269N $n = 6$	5.6 ± 1.3	–	235 ± 58	3.4 ± 0.2
WT $n = 12$[a]	–	657 ± 53	6.6 ± 1.0	0.9 ± 0.3

[a] Abell and Villafranca (1991).

Table 4: Steady-State Kinetic Parameters for H269 Mutants with Mn^{2+} at pH 6.5

enzyme	K_{mATP} (μM)	K_{mGlu} (mM)	k_{cat}[a] (s^{-1})
WT $n = 2$[b]	1.5 ± 0.3	0.071 ± 0.005	2.0 ± 0.2
H269N $n = 2$	5.3 ± 0.7	4.7 ± 0.7	2.5 ± 0.1
H269N $n = 6$	4.7 ± 0.3	2.4 ± 0.5	2.3 ± 0.2
WT $n = 12$[b]	55 ± 3	3.4 ± 0.02	5.2 ± 1.0[c]
H269N $n = 12$	250 ± 20	181 ± 32	4.1 ± 0.2[c]
H269Q $n = 5$	0.6 ± 0.1	0.070 ± 0.007	0.012 ± 0.001
H269E $n = 3$	1.2 ± 0.2	92 ± 6	0.028 ± 0.001
H269D $n = 10$	32 ± 3	–	0.06 ± 0.001
H269D $n = 2$	18 ± 2	–	0.06 ± 0.001

[a] Based on concentration of unadenylylated subunits. [b] Abell and Villafranca (1991). [c] Based on concentration of adenylylated subunits.

With Mn^{2+} as the activating metal ion however, the K_m for ATP increased only slightly compared to WT. A larger increase in the K_m for glutamate is observed; however, k_{cat} is identical to WT regardless of the adenylylation state (Table 4). Thus, with Mn^{2+} as the activating metal ion, H269N appears to be a reasonably good catalyst compared to WT.

The double reciprocal plots from the initial kinetic measurements conducted on H269N $n = 6$ with Mn^{2+} at pH 6.5 are biphasic. The plots are concave downward at concentrations of ATP > 1 mM or glutamate concentrations greater than 20 mM, indicating apparent substrate activation. The biphasic H269N $n = 6$ data may be explained by examining the kinetic constants of both the adenylylated and unadenylylated forms of the enzyme. At lower ATP concentrations (over the range of $1-100$ μM), activity is observed for only the unadenylylated subunits. As the substrate concentration increases beyond this range, the adenylylated subunits also become active. Since the adenylylated subunits turn over at a faster rate than the unadenylylated subunits, a large increase in activity is observed, producing double reciprocal plots that are concave downward. Analysis of the portion of the curve at low substrate concentrations produced the kinetic constants for H269N $n = 6$ in Table 3. The K_m values for substrates and the k_{cat} based on unadenylylated subunit concentration are in good agreement with those found for the lower adenylylation state H269N $n = 2$. This result indicates that for GS of a given adenylylation state, with Mn^{2+} as the activating metal ion, the K_m values for the tighter binding subunits (in this case it is the unadenylylated subunits) will be measured. Also the extent of adenylylation does not affect the binding

of substrates nor the turnover of the unadenylylated subunits in the steady-state.

Steady-State Kinetic Parameters—H269E and H269Q. The low adenylylation state forms of these mutants show no significant activity with Mg^{2+} (<0.0004 s^{-1} with 100 mM $MgCl_2$, 5 mM ATP, and 400 mM glutamate at pH 6.5 or 7.5) but are active with Mn^{2+}. Completely adenylylated forms of these mutants are not active with either metal. The kinetic constants summarized in Table 4 therefore reflect the activity of the unadenylylated subunits only. H269Q had K_m values for ATP and glutamate that are comparable to those of WT $n = 2$. Normally, in a case such as this, the possibility of contamination of the mutant with WT would be difficult to disprove. However, H269Q does not exhibit activity with Mg^{2+}. Since the activity of WT with Mg^{2+} is 10-fold greater than that with Mn^{2+}, if contamination with WT was the reason for the similar K_m values but reduced k_{cat}, the preparation should have shown easily detectable activity with Mg^{2+}. The possibility of WT contamination may be safely eliminated. The opportunity presents itself to study a mutant that has similar K_m values compared to WT but a reduced k_{cat} value.

In contrast to H269Q, H269E has a highly elevated K_m for glutamate (Table 4) but, unlike H269D, still allows glutamate to bind. The ability of the enzyme to bind glutamate efficiently is greatly, though not completely, restored by the double mutant E129H/H269E. In this mutant, the ligands to the n_2 metal are returned to the WT composition of two glutamates and one histidine; however, their position in space have been altered. Still the overall electrostatic environment around the n_2 metal ion now more closely resembles that of WT, and in this double mutant the K_m for glutamate is reduced to 7 mM (Wittmer et al., 1994a,b); however, k_{cat} is not restored. These results illustrate the role of the n_2 metal ion in providing an electropositive shield to facilitate the proximal binding of the γ phosphoryl group of ATP and the γ carboxylate of glutamate. With the addition of an extra negative charge at this site in the form of Glu-269, the effective positive charge of the metal is reduced, making the binding of glutamate and the formation of the γ glutamyl phosphate intermediate more difficult as evidenced by the elevated K_m for glutamate and the reduced k_{cat}.

The dependence of mutant activity on the metal ion used for activation may give some indication of subtle differences in the amino acid side chains involved in catalysis for the Mn^{2+} versus the Mg^{2+} activated enzyme. The fact that mutations at histidine-269 result in large decreases in activity with Mg^{2+} as the activating metal implies that, in addition to serving as a metal ligand, the residue may be participating as an acid/base catalyst. Its role in catalysis may be somewhat less important in the presence of Mn^{2+}.

Rapid-Quench Experiments—Biosynthetic Reaction. Using the biosynthetic reaction for the rapid quench studies, it was possible to examine the effect of the metal ligand on phosphoryl transfer by studying H269N and H269Q. Quench-flow experiments were conducted with all substrates present at 5 to 10 times the K_m values measured in the steady-state experiments. Experiments were conducted at 10 °C for comparison with previous measurements with WT. For H269N, the substrate concentrations were chosen to maintain saturating conditions for the unadenylylated subunits and to minimize any contribution to the observed activity from the

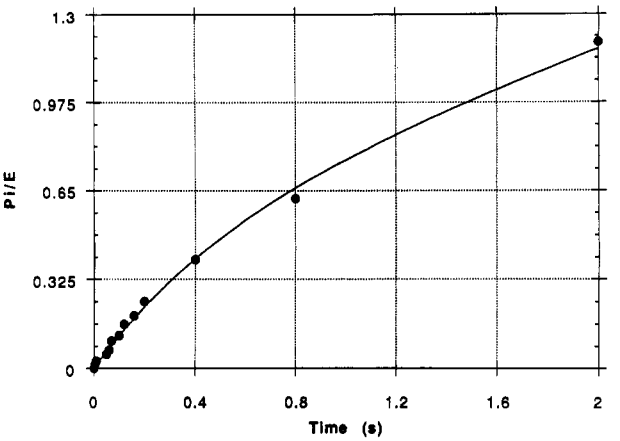

FIGURE 1: Time course of the quench flow kinetic experiment with H269N $n = 4$ at 10 °C. The final reaction mixture contained 36.5 μM unadenylylated subunits, 8 mM $MnCl_2$, 490 μM ATP, 375 μM glutamate, and 50 mM NH_4Cl at pH 6.5. The reaction was followed from 5 ms to 4 s. Data from 5 ms to 2 s are shown. (●) The actual experimental data; (—) the fit to eq 4 using the parameters given in Table 5 and the complete data set.

Table 5: Rate Constants for the Biosynthetic Reaction with Mn^{2+} at pH 6.5

constant	WT $n = 2$[a]	H269N $n = 4$	H269Q $n = 5$
A	0.68 ± 0.02	0.50 ± 0.05	–
λ (s^{-1})	6.4 ± 0.4	1.88 ± 0.27	–
k_{ss} (s^{-1})	0.47 ± 0.01	0.34 ± 0.02	0.0011 ± 0.0002
k_3 (s^{-1})	4.8	1.3	0.0011
k_4 (s^{-1})	1.0	0.09	–
k_5 (s^{-1})	0.62	0.5	–
k_3/k_4	5	15	–

[a] Abell and Villafranca (1991a).

adenylylated subunits. The K_m values for ATP and glutamate for the unadenylylated subunits of H269N are different enough from those of the adenylylated subunits to allow a fairly complete separation of the two activities. The time course of the reaction shown in Figure 1 was followed from 5 ms to 4 s. The data were fit to eq. 4 and the results are summarized in Table 5. A burst amplitude of 0.50 is observed. This amplitude is quite similar to that of 0.57 previously observed for WT $n = 2$ under the same conditions (Abell & Villafranca, 1991a).

The results of the rapid quench experiments may be related to rate constants in the biosynthetic reaction for glutamine synthetase by the analysis utilized by Meek et al. (1982). The results of these calculations are summarized in Table 5. For H269N, the interaction between the n_2 metal ion and the amide of asparagine would be expected to be weaker than the corresponding interaction with histidine. The effect of this weakened interaction appears as a slight decrease in the forward phosphoryl transfer rate; however, the most pronounced effect appears in k_4, which is the rate constant for reverse phosphoryl transfer. Compared to WT, k_4 is an order of magnitude slower for H269N, indicating that once the phosphoryl transfer to form the γ-glutamyl phosphate intermediate has occurred, the geometry is unfavorable for glutamate and ATP to reform.

In contrast to these results, the time course for the quench flow experiments with H269Q shows no burst of acid-labile phosphate. A plot of P_i/E versus time is linear over the range of 1 to 600 s. Measurements conducted at times of less than 1 s do not produce a significant amount of inorganic

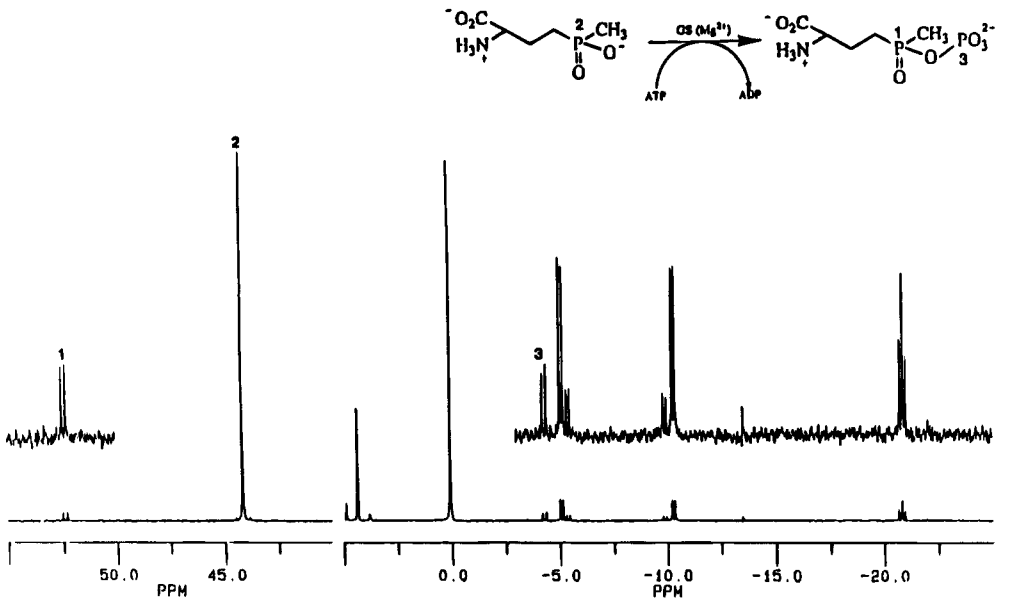

FIGURE 2: ^{31}P NMR spectrum of glutamine synthetase incubated with PPT and ATP. The data are from an incubation experiment with H269E as described in Experimental Procedures. The ^{31}P NMR spectrum was collected on a Bruker WM-360 spectrometer at 145.81 MHz using a 5 mm sample tube with broad-band (Waltz) decoupling of protons. A 32 K data set was collected with an acquisition time of 1.1 s and a receiver delay of 4 s. The spectrum represents collection of 10 000 transitions. The peaks at −5.34 and −9.92 ppm are from ADP, and the peaks at −5.28, −10.30, and −20.95 ppm are from ATP.

phosphate. The absence of a measurable burst indicates that the phosphoryl transfer step or some step prior to phosphoryl transfer such as a conformational change is rate limiting. The rate of phosphoryl transfer, 0.0011 s^{-1}, was obtained from the slope of the plot of P_i/E versus time. Glutamine in position 269 does not interfere with the K_m for ATP and glutamate compared with WT; however, in the steady state k_{cat} is severely reduced. This result is mirrored in the rapid quench data. It would appear that a small change in geometry at position 269 can greatly alter the phosphoryl transfer rate in the biosynthetic reaction.

Rapid quench experiments with the biosynthetic reaction for H269E could not be conducted under saturating conditions since the K_m for glutamate is too high (92 mM). Phosphoryl transfer for this mutant was investigated using PPT.

Trapping of PPT-P. In all cases, the resulting ^{31}P NMR spectrum was similar to that produced from WT reactions indicating that PPT-P is produced by all the mutants tested. The spectra show two sets of doublets; one centered at 52.40 ppm (J = 27.08 Hz, α-PPT-P) and the other at −4.28 ppm (J = 26.99 Hz, β-PPT-P) (Figure 2). The coupling constants between the phosphinate and phosphate are consistent with the values observed for the phosphonic acid analogue of glutamate, 2-amino-4-phosphonobutyric acid, which is phosphorylated and released by GS (Logusch et al., 1990).

Rapid Quench Experiments—PPT. In contrast to the biosynthetic rapid quench experiments, these experiments were conducted at 25 °C, thus indicating that phosphoryl transfer to glutamate is faster than that to PPT. This result is reasonable since the enzyme does not transfer a phosphoryl group to a tetrahedral intermediate during conversion of glutamate to glutamine. The data for H269E are presented in Figure 3. The data were fit to eq 5 and the results are given in Table 6. P_i/E is limited at longer reactions times by the internal equilibrium constant for phosphoryl transfer and therefore is less than 1.0. The data was also fit to the model shown in Scheme 2 using KINSIM simulations

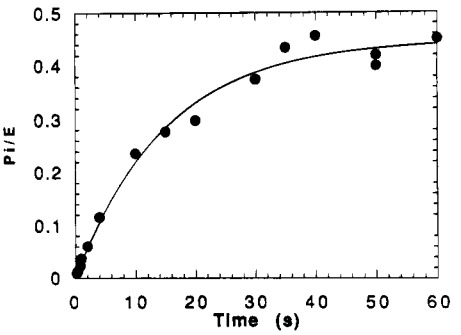

FIGURE 3: Rapid quench data for H269E with PPT in the presence of Mn^{2+} at pH 6.5 and 25 °C. Reaction conditions were as described in Experimental Procedures. Data were collected from 1 to 60 s. (●) The actual experimental data; (—) the fit to eq 5 using the parameters given in Table 6.

Table 6: Rate Constants from Fitting PPT Rapid Quench Data

enzyme	k_6 (s^{-1})	k_7 (s^{-1})	k_6/k_7
WT n = 2, Mg^{2+}[a]	5.8 ± 0.4	3.6 ± 0.5	1.6
WT n = 2, Mn^{2+}[a]	58.7 ± 5.2	24.3 ± 5.1	2.4
WT n = 12, Mn^{2+}[a]	8.6 ± 0.7	8.4 ± 1.2	1.0
H269N n = 4, Mn^{2+}	8.6 ± 1.2	4.7 ± 1.2	1.9
H269Q n = 5, Mn^{2+}	7.3 ± 1.0	5.7 ± 1.4	1.3
H269E n = 3, Mn^{2+}	0.030 ± 0.003	0.035 ± 0.008	0.84

[a] Data used for calculations were from Abell and Villafranca (1991b).

(Barshop et al., 1983). These fits produced rate constants for k_6 and k_7 that were in agreement with those shown in Table 6. KINSIM simulation fits of the data were smoother than those obtained via the nonlinear least squares solution of eq 5 which tended to overestimate k_6. However, the overestimation was not greater than 1 s^{-1} and did not change the internal equilibrium constant substantially.

Previous analysis of WT-PPT rapid quench data (Abell & Villafranca, 1991b) using KINSIM simulations only, had suggested a more complex mechanism whereby negative cooperativity had to be invoked to fit the data sufficiently. The current model, however, fits the data well without

invoking a complex mechanism for inactivation. The problem with the previous analysis, which led to the conclusion that the inactivation was occurring at different rates within the enzyme population, is likely the result of trying to fit data where the enzyme concentration and inhibitor concentrations were comparable. Such data was ignored in the current analysis. The previous analysis was insensitive to the reverse rate constants, and thus no estimate of the internal equilibrium for phosphoryl transfer could be obtained. While the relative rates of phosphoryl transfer determined from the two models is comparable, the current model is much more satisfying in that a simpler mechanism for inactivation may be used to model the data and an internal equilibrium for phosphoryl transfer is defined.

Unlike phosphoryl transfer in the biosynthetic reaction, mutation of histidine-269 to either asparagine or glutamine does not significantly alter phosphoryl transfer rates to PPT compared with WT. In addition, the internal equilibrium for this reaction (k_6/k_7) is relatively insensitive to neutral mutations.

The results of rapid quench experiments with H269E and PPT can be analyzed in both kinetic and thermodynamic terms. From a kinetic standpoint, the extra negative charge around the n_2 metal ion contributed by glutamate-269 weakens interactions between the metal ion and the reactants in the transition state for phosphoryl transfer, as indicated by the greatly reduced rate of phosphoryl transfer. A weakened interaction between the n_2 metal ion and the ADP leaving group could result in a reduced rate of phosphoryl transfer, as the ability of the metal ion to make ADP a better leaving group (Herschlag & Jencks, 1989) is now greatly compromised.

From a thermodynamic standpoint, replacement of histidine-269 with glutamate only slightly shifts the internal equilibrium to favor the enzyme−ATP−PPT complex over the enzyme−ADP−PPT-P complex. The internal equilibrium remains near unity because the interaction of the n_2 metal ion with ATP and ADP is equally affected, and thus the energies of the intermediate complexes on either side of the phosphoryl transfer transition state are affected roughly to the same extent. Crystal structures of WT with ATP or ADP show that in each complex two of the phosphorus oxygens of the substrates interact with the n_2 metal ion (Liaw & Eisenberg, 1994). Histidine-269 remains ligated to the metal ion in both structures, and thus the presence of glutamate at this position should weaken the n_2 metal interaction with either substrate.

In sum, the data presented in this paper support a direct role for the n_2 metal ion in the phosphoryl transfer reaction catalyzed by glutamine synthetase. The electrostatic environment of the metal ion at this site can be compromised by altering a neutral ligand to a negatively charged ligand, resulting in charge repulsion between the substrates and destabilization of the transition state for phosphoryl transfer.

REFERENCES

Abell, L. M., & Villafranca, J. J. (1991a) *Biochemistry 30*, 1413−1428.

Abell, L. M., & Villafranca, J. J. (1991b) *Biochemistry 30*, 6135−6141.

Almassy, R. J., Janson, C. A., Hamlin, R., Xuong, N.-H., & Eisenberg, D. (1986) *Nature 323*, 304−309.

Anderson, K. S., Sikorski, J. A., Benesi, A. J., Johnson, K. A. (1988) *J. Am. Chem. Soc. 110*, 6577−6579.

Atkins, W. M., Stayton, P. S., & Villafranca, J. J. (1991) *Biochemistry 30*, 3406.

Backman, K., Chen, Y.-M., & Magasanik, B. (1981) *Proc. Natl. Acad. Sci. U.S.A. 78*, 3743−3747.

Barshop, B. A., Wrenn, R. F., & Frieden, C. (1983) *Anal. Biochem. 130*, 134.

Cleland, W. W. (1979) *Methods Enzymol. 63*, 103.

Denton, M. D., & Ginsburg, A. (1969) *Biochemistry 8*, 1714−1725.

Hennig, S. B., & Ginsburg, A. (1971) *Arch. Biochem. Biophys. 144*, 611.

Herschlag, D., & Jencks, W. P. (1987) *J. Am. Chem. Soc. 109*, 4665−4674.

Herschlag, D., & Jencks, W. P. (1989) *J. Am. Chem. Soc. 112*, 1942−1950.

Hunt, J. B., Symyrnoitis, P. S., Ginsburg, A., & Stadtman, E. R. (1975) *Arch. Biochem. Biophys. 166*, 102−124.

Jencks, W. P. (1969) *Catalysis in Chemistry and Enzymology* pp 112−116, McGraw-Hill, New York.

Johnson, K. A. (1986) *Methods Enzymol. 134*, 677.

Kunkel, T. A., Bebenek, K., & McClary, J. (1991) *Methods Enzymol. 204*, 125−139.

Lanzetta, P. A., Alvarez, L. J., Reinach, P. S., & Candia, O. A. (1979) *Anal. Biochem. 100*, 95−97.

Lewis, D. A., & Villafranca, J. J. (1989) *Biochemistry 28*, 8454.

Liaw, S.-H., & Eisenberg, D. (1994) *Biochemistry 33*, 675−681.

Liaw, S.-H., Villafranca, J. J., & Eisenberg, D. (1993) *Biochemistry 32*, 7999−8003.

Logusch, E. W., Walker, D. L., MacDonald, J. F., Franz, J. E., Villafranca, J. J., DiIanni, C. L., Colanduoni, J. C., Li, B., & Schineller, J. B. (1990) *Biochemistry 29*, 366−372.

Meek, T. D., Johnson, K. A., & Villafranca, J. J. (1982) *Biochemistry 21*, 2158−2166.

Miller, R. E., Shelton, E., & Stadtman, E. R. (1974) *Arch. Biochem. Biophys. 163*, 155.

Morrison, J. F. (1979) *Methods Enzymol. 63*, 257.

Ninfa, A. J., & Magasanik, B. (1986) *Proc. Natl. Acad. Sci. U.S.A. 83*, 5909−5913.

Pesole, G., Bozzetti, M. P., Lanave, C., Preparatu, G., Saccone, C. (1991) *Proc. Natl. Acad. Sci. U.S.A. 88*, 522−526.

Reitzer, L. J., & Magasanik, B. (1987) in *Escherichia Coli and Salmonella Typhimurium: Cellular and Molecular Biology* (Neidhardt, F. C., Ingraham, J. L., Low, K. B., Magasanik, B., Schaechter, M., & Umbarger, H. E., Eds.), Vol. 1, pp 302−320, American Society for Microbiology, Washington, D.C.

Rhee, S. G., Chock, P. B., & Stadtman, E. R. (1985) *Methods Enzymol. 113*, 213.

Roseman, J. E., & Levine, R. L. (1987) *J. Biol. Chem. 262*, 2101.

Sayers, J. R., & Eckstein, F. (1988) in *Genetic Engineering: Principles and Methods* (Setlow, J. K., Ed.) Vol. 10, p 109, Plenum Press, New York.

Villafranca, J. J., & Waller, F. C. (1974) *Biochemistry 13*, 3286−3291.

Villafranca, J. J., Ash, D. E., & Wedler, F. C. (1976) *Biochemistry 15*, 536−543.

Witmer, M. R., Palmieri-Young, D., & Villafranca, J. J. (1994a) *Tech. Protein Chem. 5*, 321.

Witmer, M. R., Palmierei-Young, D., & Villafranca, J. J. (1994b) *Protein Sci. 3*, 1746.

Woolfolk, C. A., Shapiro, B. M., & Stadtman, E. R. (1966) *Arch. Biochem. Biophys. 116*, 177.

Yamashita, M. M., Almassy, R. J., Janson, C. A., Cascio, D., & Eisenberg, D. (1989) *J. Biol. Chem. 264*, 17681−17690.

BI951347V